HOKKAIDO UNIVERSITY

Title	Localization of the Nitric Oxide/cGMP Signaling Pathway-Related Genes and Influences of Morpholino Knock-Down of Soluble Guanylyl Cyclase on Medaka Fish Embryogenesis
Author(s)	Yamamoto, Takehiro; Yao, Yuko; Harumi, Tatsuro et al.
Citation	Zoological Science, 20(2), 181-191 https://doi.org/10.2108/zsj.20.181
Issue Date	2003-02
Doc URL	https://hdl.handle.net/2115/32961
Rights	(c) 日本動物学会 / 本文献の公開は著者の意思に基づくものである
Type	journal article
File Information	http___www.jstage.jst.go.pdf20(2)181.pdf

Hokkaido University Collection of Scholarly and Academic Papers : HUSCAP

ZOOLOGICAL SCIENCE **20**: 181–191 (2003)
© 2003 Zoological Society of Japan

Localization of the Nitric Oxide/cGMP Signaling Pathway–Related Genes and Influences of Morpholino Knock-Down of Soluble Guanylyl Cyclase on Medaka Fish Embryogenesis

Takehiro Yamamoto[1], Yuko Yao[1], Tatsuro Harumi[2] and Norio Suzuki[1]*

[1]*Division of Biological Sciences, Graduate School of Science, Hokkaido University, Sapporo 060-0810, Japan*
[2]*Department of Anatomy, Asahikawa Medical College, Asahikawa 078-8510, Japan*

ABSTRACT—To better understand the nitric oxide (NO) / cyclic GMP (cGMP) signaling pathway during embryogenesis, we examined the spatial and temporal expression pattern of the genes for neuronal nitric oxide synthase (*nNOS*), soluble guanylyl cyclase (soluble GC) subunit (*OlGCS-α_1*, *OlGCS-α_2*, and *OlGCS-β_1*), and cGMP-dependent protein kinase (cGK) I and II (*cGK I* and *cGK II*) in the medaka fish embryos. *OlGCS-β_1* and *nNOS* were expressed maternally and *OlGCS-α_1*, *OlGCS-α_2*, *cGK I*, and *cGK II* were expressed zygotically. The zygotic expression of *OlGCS-α_1* and *cGK I* was detected at stage 19, while that of *OlGCS-α_2* was detected at stage 16. Whole-mount *in situ* hybridization showed that the expression of *nNOS* or *cGK I* was localized in tail bud, otic vesicles, thyroid, and brain ventricle, or in thymus, gill arch, and olfactory pits, respectively, and that of *OlGCS-α_1*, *OlGCS-α_2*, or *OlGCS-β_1* was dim and dispersed throughout the embryos. To clarify the "role of the NO/cGMP signaling pathway in embryogenesis, we examined the influences of morpholino antisense oligonucleotide of the soluble GC subunit gene (α_1-MO, α_2-MO or β_1-MO) on development of medaka fish embryos. Embryos injected with α_1-MO or α_2-MO mainly exhibited abnormalities in the central nervous system, including defects in the formation of forebrain, eye, and otic vesicles. α_2-MO injection caused cell death at the tail bud of the embryos at stage 22, and β_1-MO injection inhibited the development of the embryos at late blastula. These results suggest that the NO/cGMP signaling pathway plays critical roles in early embryogenesis.

Key words: NO, soluble guanylyl cyclase, *in situ* hybridization, development, morpholino

INTRODUCTION

There is increasing evidence that the nitric oxide (NO)/cGMP signaling pathway plays an essential role in signal transduction in various biological systems e.g., cardiovascular regulation, immune response, and neuronal long-term potentiation via modulator molecules such as NO synthase (NOS), soluble guanylyl cyclase (soluble GC), cGMP-dependent phosphodiesterase (PDE), cyclic nucleotide-gated (CNG) cation channel, and cGMP-dependent protein kinase (cGK) (Schmidt and Walter, 1994; Kusakabe and Suzuki, 2000; Lucas *et al*., 2000).

Three distinct isoforms of NOS are known: two constitutive types (neuronal NOS, nNOS and endothelial NOS, eNOS) and an inducible type (inducible NOS, iNOS) (Marsden *et al*., 1993; Hall *et al*., 1994; Chartrain *et al*., 1994). It has been reported that knock out of *iNOS* caused an increased susceptibility to infection in mice with intracellular pathogens and a blunted hypotensive response to lipopolysaccharide (LPS) (MacMicking *et al*., 1995; Wei *et al*., 1995) and that knock out of *eNOS* caused hypertension in null mice (Huang *et al*., 1995; Lee *et al*., 2000), although the *nNOS*-deficient mice displayed almost normal morphologically (Huang *et al*., 1993). In most of these cases, however, the presence of a compensation system among isoforms is suspected, and thus it has been difficult to come to a detailed understanding of the roles of NO *in vivo*.

Soluble GC, a key enzyme in the NO/cGMP signaling pathway, is activated by NO generated from L-arginine by NOS and catalyzes the conversion of GTP to cGMP. Soluble GC is a heme-containing heterodimeric enzyme composed of α and β subunits. In mammals, four soluble GC subunit cDNAs (α_1, α_2, β_1, and β_2) have been isolated from various tissues (Koesling *et al*., 1988, 1990; Yuen *et al*.,

* Corresponding author: Tel. +81-11-706-4908;
FAX. +81-11-706-4461.
E-mail: norio-s@sci.hokudai.ac.jp

1990; Harteneck *et al*., 1991). It has been demonstrated that either α_1/β_1 or α_2/β_1 heterodimeric protein is an active enzyme in the expression system (Russwurm *et al*., 1998), although the variation of the activated dimer (α_1/β_1 or α_2/β_1) *in vivo* remains to be clarified. In previous studies, we isolated the cDNA and genomic DNA clones encoding the soluble GC subunit genes, *OlGCS-α_1* and *OlGCS-β_1*, both of which are aligned tandemly on the genome of the medaka fish *Oryzias latipes* (Mikami *et al*., 1998, 1999), and in a more recent study we demonstrated that the proximal promoter regions in the 5'-flanking regions of both subunit genes mutually influenced each other's promoter activity (Yamamoto and Suzuki, 2002).

Two distinct isoforms (cGK I and cGK II) of cGKs which are the major targets of cGMP have been identified in mammals (Wernet *et al*., 1989). cGK I is expressed mainly in smooth muscle, platelets, and the cerebellum (Butt *et al*., 1993). Loss of the *cGK I* gene abolishes NO/cGMP-dependent relaxation of smooth muscle, resulting in severe vascular and intestinal dysfunction (Pfeifer *et al*., 1998). The *cGK II* gene is expressed in the intestine, kidney, brain, and bone (Markert *et al*., 1995), and mice deficient in *cGK II* have been shown to be resistant to the heat-stable enterotoxin (STa) and to display dwarfism owing to a severe defect in endochondral ossification at the growth plate (Pfeifer *et al*., 1996).

Despite the growing body of information on these modulator molecules, soluble GC knock-out mice have not yet been established and to our knowledge, however, the roles of the NO/cGMP signaling pathway during early embryogenesis have not been well investigated. On the other hand, morpholino antisense oligonucleotides (MOs) have been shown to efficiently knock-down the translation of various genes in zebrafish embryos (Nasevicius and Ekker, 2000). In addition, in a wide range of model organisms, as well as in zebrafish, sea urchins, ascidians, frogs, chicks, and mice, MOs have been specifically designed to overcome many of the limitations of regular DNA oligos, such as their specificity for the target mRNA, stability, and toxicity. Accordingly, we here investigated the spatial and temporal expression patterns of several genes in this pathway, *i.e*., *nNOS*, *OlGCS-α_1*, *OlGCS-α_2*, *OlGCS-β_1*, *cGK I*, and *cGK II* by means of *in situ* hybridization using the medaka fish *O. latipes* as a vertebrate model. In addition, we performed a knock-down of soluble GC to block the NO/cGMP signaling pathway with the latest loss-of-function technology. MOs-injected embryos exhibited the defects presumed from the investigation of knock-out mice mentioned above, such as abnormal development of the CNS and eyes, and also they showed cell death in the tail bud, enlarged otic vesicles, and a reduced number of blood cells.

MATERIALS AND METHODS

Animals and embryos

Adults and embryos of the orange-red variety of the medaka fish *O. latipes* were maintained as described by Yamagami *et al*. (2001). The developmental stage was expressed in the manner described by Iwamatsu (1994). Total RNA was prepared from the embryo, fry, or various adult organs of the medaka fish *O. latipes* using TRIzol reagent (Invitrogen, Carlsbad, CA, USA).

Cloning of cDNA fragments of medaka fish *nNOS*, *cGK I*, and *cGK II* by RT-PCR

The degenerate oligonucleotides were designed based on seven amino acids conserved in all reported NOS protein sequences (N-deg.1: 5'-CCYGTBTTCCAYCAGGAGATG-3' for amino acid sequence PVFHQEM; N-deg.2: 5'-RAAGGCRCAR-AASTGRGGGTA-3' for amino acid sequence TP(H/Q)FCAF). First PCR amplification was carried out with first strand cDNA of whole fry as a template and performed for 30 cycles. Denaturation, annealing, and elongation reactions were carried out at 96°C for 30 sec, 50°C for 30 sec, 72°C for 60 sec, respectively. A second PCR was then performed with the nested primers designed based on the sequence conserved in salmon and zebrafish *nNOS* genes (Holmqvist *et al*., 2000; Øyan *et al*., 2000)(N-3:5'-CAGGAGATGCTCAAC-TATC-3', N-4: 5'-TCCAGTGCTCTCGAAGTTG-3') under the same conditions as used for the first reaction.

A medaka fish *cGK I* cDNA fragment was obtained by RT-PCR using primers constructed based on the zebrafish EST clones (AI722011 and AI721318); *cGK I* Fwd: 5'-ATCATCGACACCTTTG-GAGTTGG-3'; *cGK I* Rev: 5'-CACATTGTAAATGCTTTATCCA-GAG-3'. The amplification conditions were 30 sec at 96°C, 30 sec at 56°C, and 60 sec at 72°C for 30 cycles.

A cDNA fragment of *cGK II* was isolated by RT-PCR with the following primers: G2-F1, 5'- AGGAAAGGTGAAAGTCACACA-3'; G2-R1: 5'-CTGGAGTCCCACAGAATGTCCA-3'. The amplification conditions were consisted of 5 cycles of 30 sec at 96°C, 30 sec at 50°C, and, 30 sec at 72°C, followed by 30 cycles of 30 sec at 96°C, 30 sec at 55°C, and 30 sec at 72°C. Nested PCR was carried out with following primers using the first PCR product as a template: G2-F2, 5'-GAAAGGAGAGTACTTTGGAGA-3'; G2-R2, 5'-TCCCC-ACCTAAGCAGGCCTCCA-3'. The nested PCR conditions were the same as for the first PCR. The PCR product was purified and subcloned into the plasmid vector pBluescript II KS (+) (Stratagene, La Jolla, CA, USA) and sequenced.

Detection of *OlGCS-α_1*, *OlGCS-α_2*, *OlGCS-β_1*, *nNOS*, *cGK I*, and *cGK II* transcripts in medaka fish embryos by RT-PCR

First strand cDNAs were reverse-transcribed from the 4 μg total RNA obtained from various developmental stages of embryos. Primers used for RT-PCR of medaka fish soluble GC α1 subunit were as follows: α1/14-R, 5'-CTTGAAAGGTCAGATGAT-3'; α1/14F-c, 5'-ATAGACATCAAGCTCTCC-3'. Those for medaka fish soluble GC β_1 and α_2 subunits were as follows: β1/s-d2, 5'-CAAATC-CATGGAACAGAG-3'; β1/SR-1, 5'-CTTGCTGCGTAGAACAAAG-3'; α2/5'E, 5'-TTCTTTGGTGCCGGCCTGCG-3'; α2/a2TEST, 5'-CTGCACTGATTCAACCCTGG-3'. Medaka fish *nNOS* and *cGK I*, and *cGK II* cDNA fragments were amplified with the following primers: nNOS/F, 5'-TTCCTTTGAGTATCAGG-3'; nNOS/R, 5'-CAAAT-GTACTGGTCACC-3'; cGK I/F, 5'-AACATGGACTTTCTGG-3'; cGK I/R, 5'-TTGATTAGGTTACCAGC-3'; cGK II/F, 5'-CAGAGACAATT-TCAACC-3'; cGK II/R, 5'-GTCCGGAATAATCTGATG-3'. The amplification conditions were 30 sec at 96°C, 30 sec at 52°C, and 30 sec at 72°C for 30 cycles.

Microinjection of morpholino antisense oligonucleotides into medaka fish embryos

The following morpholino antisense oligonucleotides (MOs) of medaka fish soluble GC α_1-, α_2-, and β_1-subunit mRNAs were purchased from GeneTools, LLC (Corvalis, OR, USA): α_1-MO, 5'-TCTTTCAACTTGGCGCAGAACATCT-3'; α_2-MO, 5'-GATCTTGCGTGACGAAGAAGACATT-3'; β_1-MO, 5'-GGCGTGATTCACAAAACCATACATG-3'. The sequence complementary to the predicted start codon is underlined. For rigorous specificity studies, β_1-MOs with 4 mispairs (β1-4 mis MO): 5'-GGCGaGATTgACAAAtCCATtCATG-3' or mRNA of *OlGCS-α_1*, *OlGCS-α_2*, or *OlGCS-β_1* were injected into 1- or 2-cell-stage embryos. The full-length cDNAs of *OlGCS-α_1* and *OlGCS-β_1* were isolated previously (Mikami *et al*., 1998) and the *OlGCS-α_2* cDNA fragment was amplified using the following primers a2-fwd for 5'-GGTGGTACGGAGCCCGCTGTAGCA-3' and a2-rev for 5'-GAACAGCAAACATTTATATTCCAGAACTGC-3', then subcloned into pBluescript II KS (+). The mRNA was synthesized using mMESSAGE mMACHINE kit (Ambion, Austin, TX, USA). The respective MO was dissolved in phosphate buffered saline (PBS) at from 1.7 to 2.0 μg/μl, and microinjected into embryos as described previously (Mikami *et al*., 1999).

***in situ* hybridization**

The plasmid vector pBluescript II KS (+) containing the *nNOS*, *cGK I*, or *cGK II* cDNA fragments described above was used as a template for labeling the RNA probe. The *OlGCS-α_2* cDNA fragment was amplified by the primers a2-F for 5'-TGCATCCCCCTTTACCATCC-3' and a2-tail for 5'-AAATCCAAAGCTCAGCACCC-3' and subcloned into the vector. The probes for *OlGCS-α_1* and *OlGCS-β_1* were prepared as described previously (Yamamoto and Suzuki, 2002). Fixed embryos were embedded in Tissue-Tek OCT compound (Sakura Finetechnical Co., Ltd., Tokyo, Japan), and cryosectioned at 10 μm. Whole-mount *in situ* hybridization was carried out as previously described (Yamamoto and Suzuki, 2002) with some modifications. Briefly, a labeled ribo-probe was purified by RNeasy (QIAGEN, Hilden, Germany) to reduce background. Fixed and dechorionated embryos were treated with 10 μg/ml Proteinase K (Roche, Mannheim, Germany) in PBS with 0.1% tween-20 (PBST) at room temperature. The embryos were incubated in prehybridization buffer containing 50% formamide, 5xSSC, 0.1% Tween-20, 5 mg/ml yeast RNA (Sigma, Woodlands, TX, USA), and 50 μg/ml heparin (Sigma) for 1 hr at 65°C, and then hybridized with a digoxigenin-labeled RNA probe (100 ng/ml) overnight. Following the washes in 2xSSC with 0.1% tween-20 (SSCT)/50% formamide at 65°C twice, and in 2xSSCT at 65°C for 15 min, and then twice in 0.2xSSCT at 65°C for each 15 min, the embryos were incubated in the blocking solution containing 10% sheep serum (Sigma) in PBST for 1 hr at room temperature. After blocking, the embryos were incubated with 1/2000-diluted anti-digoxigenin Fab fragment (Roche) in PBST with 10% sheep serum at 4°C overnight. Following 4 washes with PBST for 30 min and 3 washes with DIG-3 buffer (0.1 M NaCl, 50 mM $MgCl_2$, 0.1M Tris-HCl, pH 9.5, and 0.1% Tween-20) for 5 min, the sample was further incubated with BM-perple (Roche) at 4°C. After the coloring reaction, the dehydrated embryos were mounted in glycerol or 2% methyl cellulose in 0.85xPBST.

Other methods

The nucleotide sequence was determined by the dideoxy chain termination method (Sanger *et al*., 1977) with an Applied Biosystem 3100 Genetic analyzer. Data was analyzed with DNASIS software (Hitachi Software Engineering Co., Yokohama, Japan) and GENETYX-MAC/version 7.2.0 (Softwere Development, Tokyo, Japan). The homology search was performed at the Web site (NCBI BLAST; http://www.ncbi.nlm.nih.gov/BLAST/) MO-injected embryos and *in situ* hybridization samples were observed under a light microscope (BX50W1, Olympus, Japan; MZ8, Leica, Switzerland).

RESULTS

Isolation of NO/cGMP pathway-related genes

In the NO/cGMP signaling pathway, NO activates soluble GC, leading to an increase of intracellular cGMP levels and to the induction of cGMP-dependent reactions mediated by such proteins as PDE, CNG channels, and cGK, as illus-

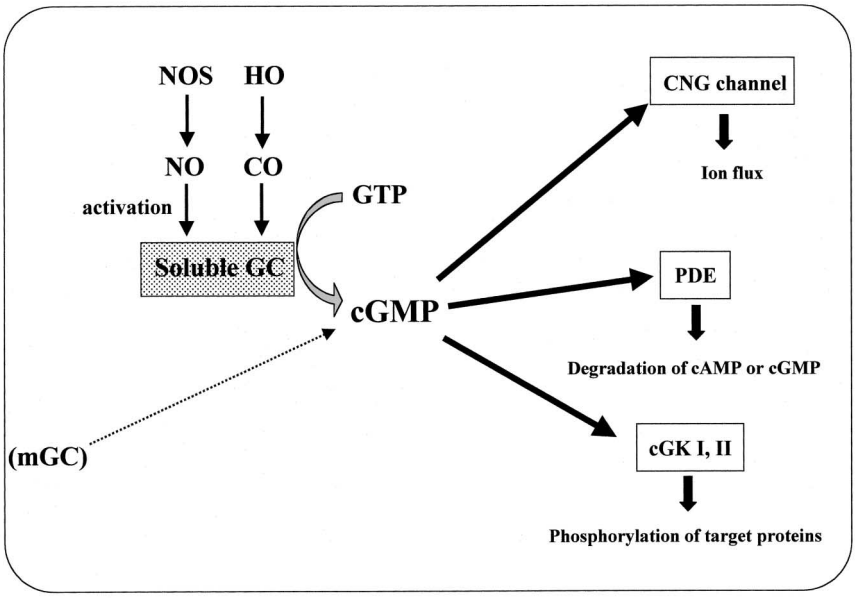

Fig. 1. A schematic drawing of the NO/cGMP pathway. Soluble GC is activated by binding of NO generated by nitric oxide synthase (NOS) or carbon monoxide (CO) catalysed by heme oxigenase (HO) to a prosthetic heme group. cGMP produced by soluble GC modulates the effectors, such as cGMP-dependent protein kinase (cGK), cyclic nucleotide-gated (CNG) cation channel, and phosphodiesterase (PDE).

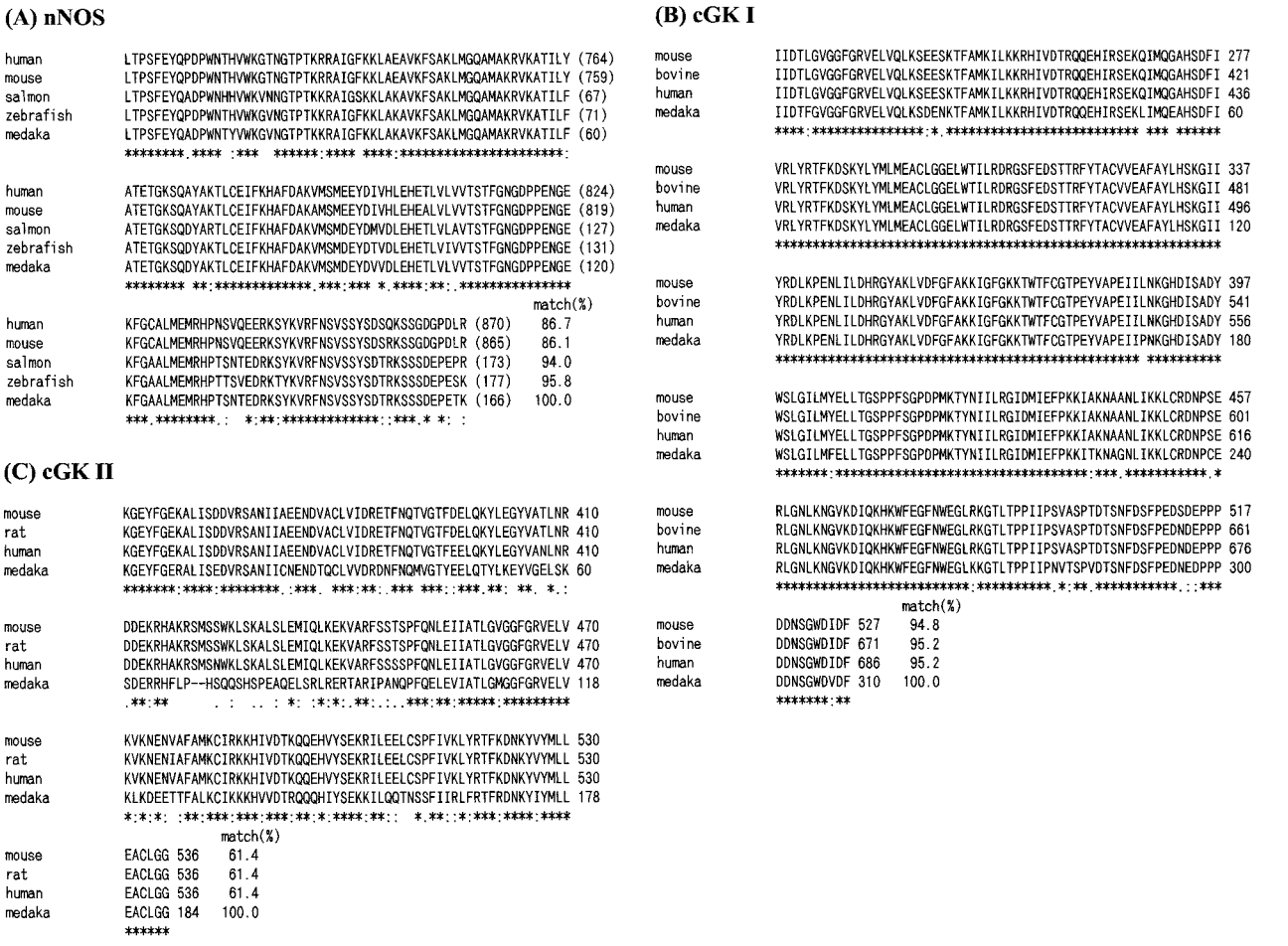

Fig. 2. Multiple alignment of the deduced amino acid sequence of the medaka fish (A) *nNOS*, (B) *cGK I*, and (C) *cGK II* genes with the amino acid sequences of the corresponding region from various species. Accession numbers are: human nNOS, NM_000620; mouse nNOS, NM_008712; zebrafish nNOS, AF219519; salmon nNOS, AJ006209; mouse cGK I, NM_011160; bovine cGK Iα, X16086; human cGK I, NM_006258; mouse cGK II, NM_008926; rat cGK II, NM_013012; human cGK II, NM_006259.

trated in Fig. 1. In the present study, we initially isolated the cDNA fragments of some of the genes participating in the pathway (*nNOS*, *cGK I*, and *cGK II*) by RT-PCR, and then examined their spatial and temporal expression patterns during embryogenesis of the medaka fish *O.latipes*.

The deduced amino acid sequence (166 amino acids) of a 502 bp cDNA fragment obtained by RT-PCR with a pair of degenerate primers (N-deg.1 and N-deg.2, N-3 and N-4) contained the calmodulin-binding domain (CaMBD) and a part of the flavin adenine mononucleotide-binding domain (FMNBD) typical in mammalian nNOS and showed about 95.8% similarity to the zebrafish nNOS, 94.0% to the salmon nNOS, and 86.7% to the human nNOS, respectively (Fig. 2A). Unfortunately, in the present study we could not obtain the other two isoforms of NOS, iNOS and eNOS, with the pair of degenerate primers.

Similarily, we obtained a 1145 bp cDNA fragment which corresponds to exon 10 to 18 of the human *cGK I* gene, and which contained a catalytic domain, an ATP-binding domain, and a carboxyl-terminal domain. The deduced 310 amino acid sequence of the cDNA fragment is 94.8% homologous

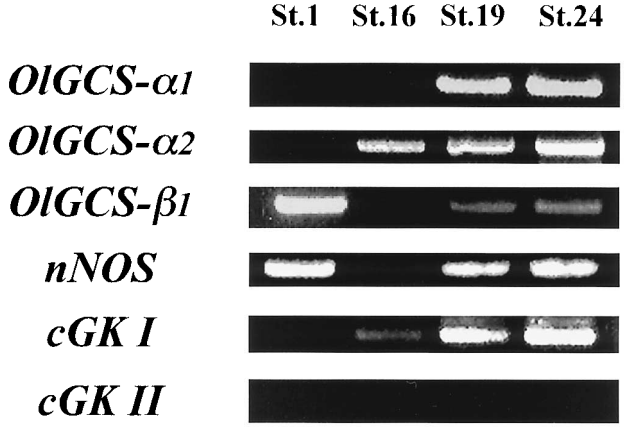

Fig. 3. RT-PCR analysis of the expression of NO/cGMP signaling pathway-related gene (*OlGCS-*α_1, *OlGCS-*α_2, *OlGCS-*β_1, *nNOS*, *cGK I*, and *cGK II*) transcripts throughout embryogenesis. Reverse transcription of total RNA (4 μg) from various developmental stages (stage 1, fertilization egg; stage 16, late gastrula stage; stage 19, 2-somite stage; stage 24, heart formation stage) was carried out using Superscript II and olido(dT)$_{12-18}$ primers. The resultant cDNAs were used for the PCR as a template. The PCR products were run on 2% agarose gels and the gels were stained with ethidium bromide.

to that of mouse cGK I and 95.2% homologous to that of bovine and human cGK I (Fig. 2B). We also obtained a 555 bp cDNA fragment of which deduced 184 amino acid sequence is similar to that of mammalian cGK II (61.4% identity; Fig. 2C).

Expression of NO/cGMP signaling pathway-related genes in the medaka fish embryos at various developmental stages

We examined the temporal expression patterns of *OlGCS-α_1*, *OlGCS-α_2*, *OlGCS-β_1*, *nNOS*, *cGK I*, and *cGK II* during embryogenesis by RT-PCR (Fig. 3). *OlGCS-β_1* and *nNOS* were detected at stage 1, indicating that they are expressed maternally. *OlGCS-α_2* was expressed at stage 16, and *OlGCS-α_1* and *OlGCS-β_1* were expressed at stage 19, indicating that they are expressed zygotically. The expression of *cGK II* could not be detected at stages16 and 19. *cGK II* was expressed at the later developmental stage (stage 32) (data not shown).

Spatial expression pattern of mRNA of NO/cGMP signaling pathway-related genes during early embryogenesis

Whole-mount and section *in situ* hybridization revealed the presence of the transcripts of *OlGCS-α_1* and *OlGCS-β_1* in the whole brain and embryonic kidney of the 7-day-old and hatched embryos, and the *OlGCS-α_2* transcript was also detected in the whole brain (Fig. 4). However, in early developing embryos the signals due to the transcripts of three soluble GC subunit genes were dispersed over the embryos. However, none of signals due to these subunit genes were detected in the embryos with sense probe (data not shown).

The expression pattern of *nNOS* mRNA was changed dynamically dependent on the developmental stage. After stage 18, the signal was detected in the tail bud (Fig. 5A-a) and at stages 21–22, the transcript also became detectable in the otic vesicles and thyroid (Fig. 5A-b). After stage 28, the signal was detected in the brain ventricle (Fig. 5A-c, d). Interestingly, the signal of the tail bud disappeared gradually

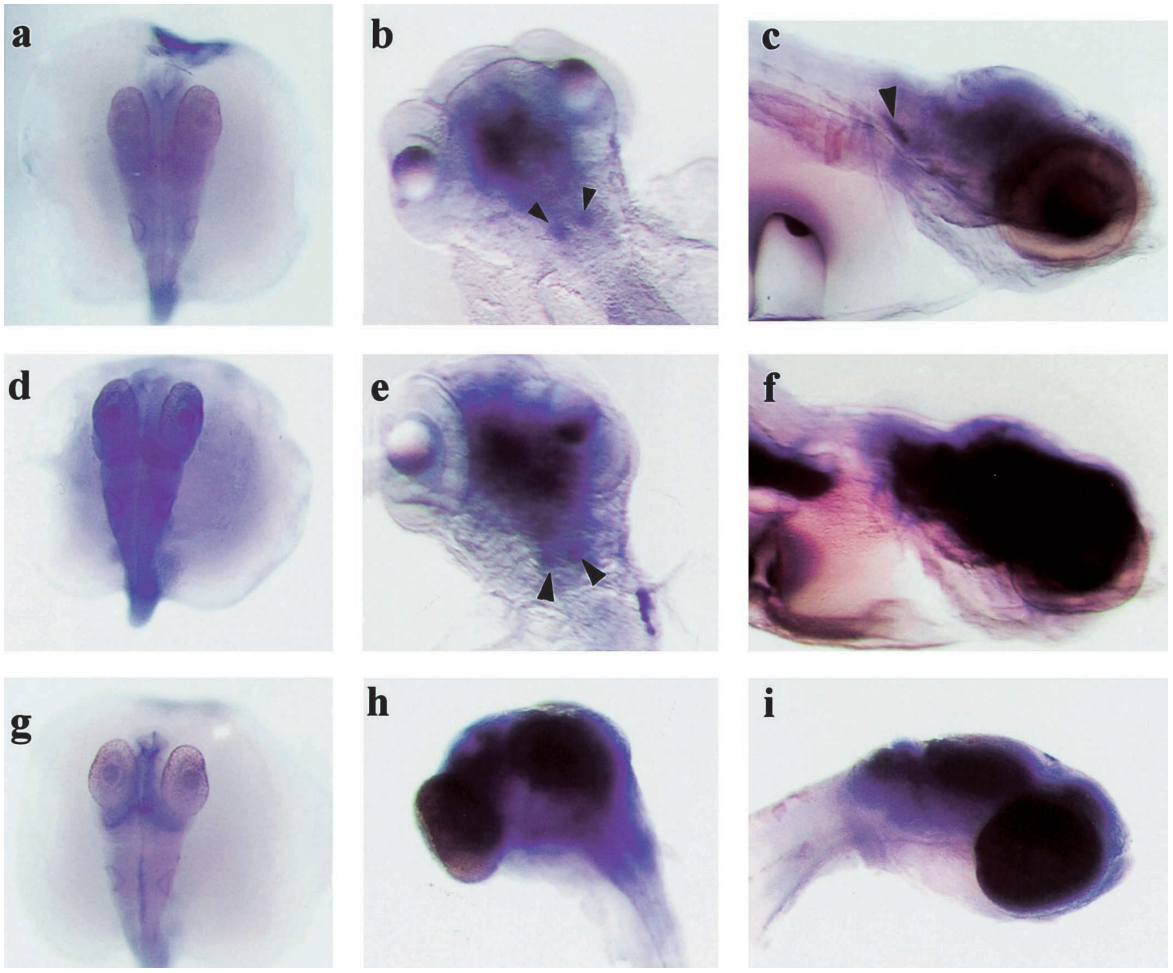

Fig. 4. Expression of the medaka fish soluble GC transcripts visualized by *in situ* hybridization. Expresson of *OlGCS-α_1* (a, b, c), *OlGCS-β_1* (d, e, f), *OlGCS-α_2* (g, h, i) transcripts are shown. Dorsal views of embryos at stage 27 are shown in (a, d, g) and those of embryos of stage 37 are shown in (b, e, h). Side views of stage 39 hatched embryos (c, f). Side view of stage 37 embryos (i). In the early developmental stage of embryos the signals corresponding to these three subunit genes were dim and dispersed throughout the embryos, and then became restricted to the brain as development continued. Arrowheads indicate the signal in the embryonic kidney.

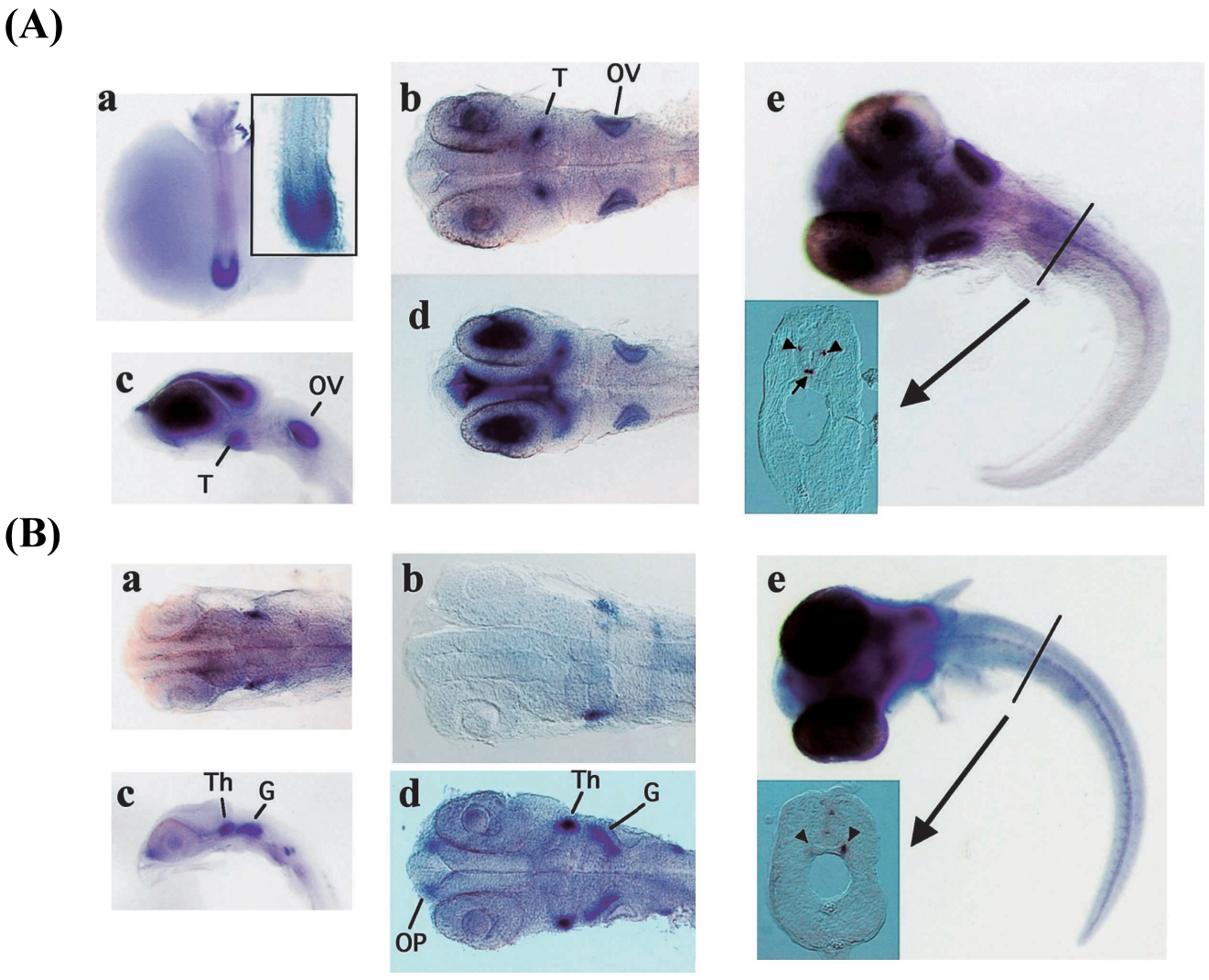

Fig. 5. Expression of NO/cGMP signaling pathway-related genes in medaka fish embryos detected by *in situ* hybridization with (A) nNOS, (B) cGK I antisense probes. (A-a),Dorsal view of a stage 22 embryo and high magnification of the tail bud. (A-b) Dorsal view of a stage 26 embryo. (A-c, d) Side view (c) and dorsal view (d) of a stage 28 embryo. (A-e) Dorsal view of 5-day-old embryos and cross section of the trunk region. The signals were detected in the neural tube floor plate (arrow) and the lateral spinal cord (arrowhead). (B-a) Dorsal view of stage 22 embryo. (B-b) Dorsal view of stage 24 embryo. (B-c, d) Side view (c) and dorsal view (d) of the stage 27 embryo. (B-e) Dorsal view of 5-day-embryos and cross section of the trunk region. The signals were detected in the dorsal root ganglion (DRG) (arrowhead). Abbreviations: G, gill arch; OP, olfactory pit; OV, otic vesicle; T, thyroid; Th, Thymus.

with development, and at stage 28 it had nearly vanished, while the other signals were still detectable at this stage. The section *in situ* hybridization using the 5-day-old embryos (around stage 35) showed that *nNOS* was prominently expressed in the spinal floor plate (Fig. 5A-e, arrow) and the lateral spinal cord (Fig. 5A-e, arrowhead).

At stage 22, the signal due to *cGK I* was detected in the lateral side (Fig. 5B-a). At stage 24, the signal was detected in the thymus and gill arch (Fig. 5B-b), and at stage 27, the signal was faintly detected in the olfactory pits (Fig. 5B-d). The section *in situ* hybridization using the 5-day-old embryos demonstrated that expression of the *cGK I* transcript was localized in the dorsal root ganglion (DRG) neurons (Fig. 5B-e). However, we could not detect the expression of *cGK II* through the all developmental stages (data not shown).

The influences of disruptions of the NO/cGMP signaling pathway by soluble GC knock- down using morpholino antisense oligonucleotide (MOs) on medaka fish embryogenesis

As described above, the expression of *nNOS* and *cGKs* tended to be tissue-specific compared with that of soluble GC subunit mRNAs, which was more disperse, suggesting that soluble GC is involved in many events in many different cells in the possible combinations of the subunits (α_1/β_1 or α_2/β_1) during early embryogenesis. To determine the phenotypes induced by the knock-down of a given soluble GC

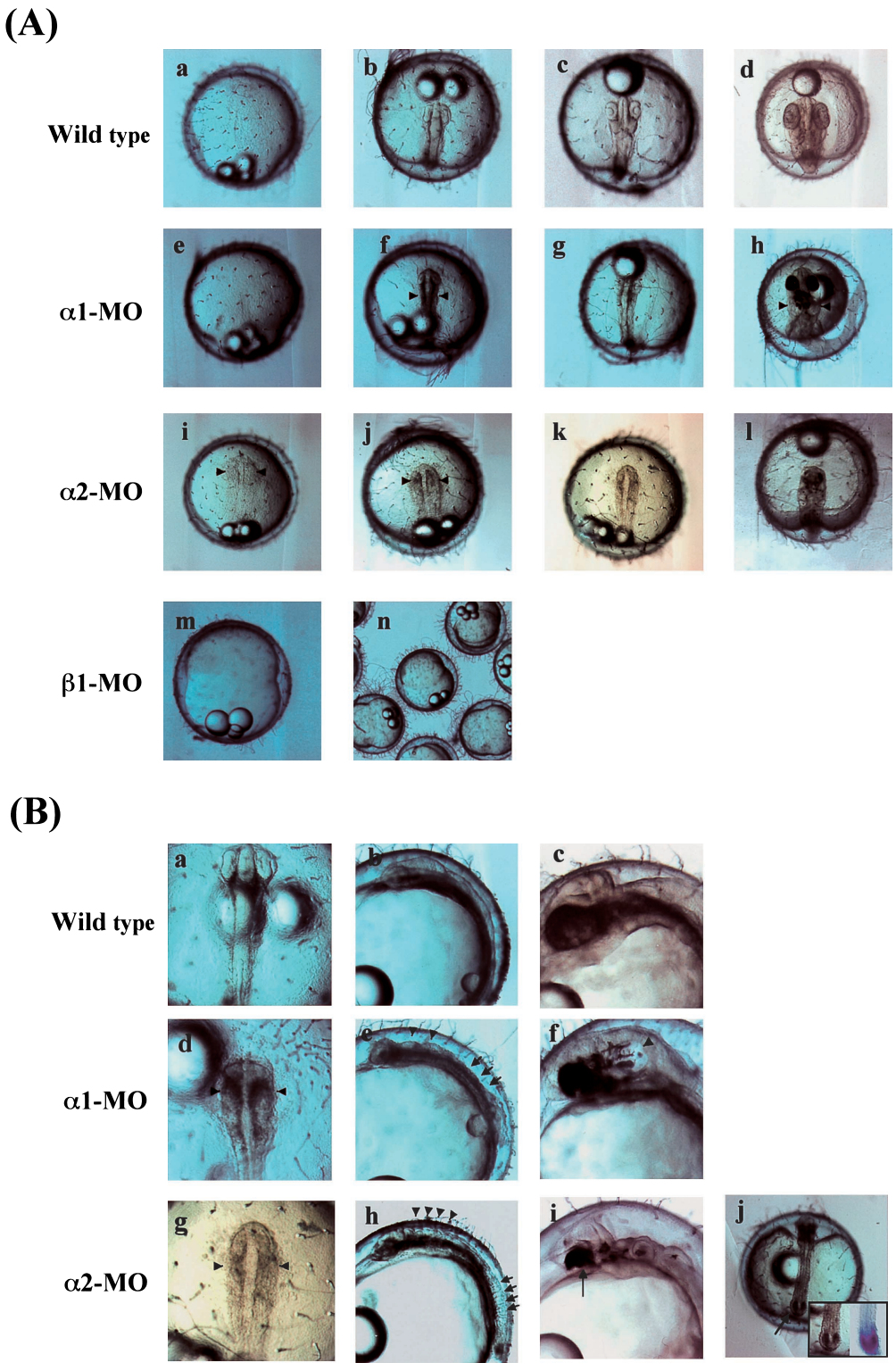

Fig. 6. Phenotypes of soluble GC knock-down embryos induced by injection of morpholino antisense oligonucleotides (MOs). (A) Development of soluble GC knock-down embryos. (a, b, c, d) Wild type embryos; (e, f, g, h) α_1-MO injected embryos; (i, j, k, l) α_2-MO injected embryos; (m, n), β_1-MO embryos. (a, e, i) stage 16, (j) stage 18, (b, f, k) stage 20, (c, g) stage 23, (d) stage 28, (h, l) 7-day-old embryos after injection. (f, i, j) Note the defects at the lateral side of embryo (arrowhead). (h) Note the enlarged otic vesicles (arrowhead). (m, n) β_1-MO injected embryos. Embryos were injected at 1.2 μg/μl and cultured at 22°C. Embryos displayed the inhibition of development around the stage 15. (B) Large magnification of soluble GC knock-down embryos. (a, b, c) Wild type embryos, (d, e, f) α_1-MO injected embryos, (g, h, i, j) α_2-MO injected embryos. Arrowheads in (d, g) indicate the defects at the lateral side of embryo. (f) Note the enlarged otic vesicles (arrowhead). (a, d, g) Dorsal views with anterior upward of stage 21 embryos. (e, h) Note the wavy notochord (arrowhead) and irregular somite border (arrow). (b, e, h) Side views of stage 21 embryos. (c, f, i) Side views of stage 30 embryos. (i) Note the fused eye at the ventral forebrain (arrow) (j) Tail defect of α_2-MO injected embryos (arrow). Right corner, large magnification of tail defect and the expression of nNOS in a wild-type embryo.

subunit gene using MOs, we designed experiments to block the formation of the α_1/β_1 or α_2/β_1 heterodimer by using a_1-MO or α_2-MO. The α_1-MO or α_2-MO injection caused nearly identical phenotypes in the medaka fish embryos. The MO-injected embryos displayed defects mainly in the CNS, for example, the formation of a slightly wavy notochord and irregular somite border (arrows and arrowheads in Fig. 6B-e and 6B-h). In addition, MO-injected embryos developed more slowly than the control embryos. When high concentrations (over 2.0 μg/μl) of MO were injected, the embryos showed the most severe phenotype, i.e. cessation of development at the state of lumps of cells. The α_1-MO injected embryos displayed the degenerated cells in the lateral side of the embryonic body at stage 17 (arrowheads in Fig. 6A-f and 6B-d) and the enlargement of the otic vesicles at 7 days after the injection (arrowheads in Fig. 6A-h and 6B-f), which may be caused by apparent cell death judging from the observation that the future tissues derived from the cells developed abnormally and the number of cells shown in Fig. 6A-f, j (arrowheads) and 6B-e, h (arrow and arrowheads) was reduced remarkably after MO injection. α_2-MO injection also caused severe defects in the embryos at the late gastrula in a manner similar to α_1-MO injection, although the defects due to α_2-MO injection appeared slightly earlier than those by α_1-MO injection, which appeared at stage 16 (arrowheads in Fig. 6A-i and 6A-j). In addition, the embryos showing severe defects also showed of abnormal development of the forebrain and eyes, with some showing formation of a cyclopean eye at the ventral forebrain (Fig. 6B-i, arrow). Amazingly, in the stage 22 embryos with mild defects, the degenerate cells were also observed at the tail bud (Fig. 6B-j, arrow). Moreover, most of the α_1-MO or α_2-MO injected embryos seemed to contain fewer blood cells than the control embryos, despite the apparently normality in formation of the blood vessels and heart. Surprisingly, the β_1-MO injected embryos displayed delay and inhibition of development after the blastula stage in a dose-dependent manner (Fig. 6A-m, 6A-n). In additon, at regular culture temperature (28°C), the β_1-MO injected embryos developed as did the α_1-MO or α_2-MO injected embryos, while at lower temperature (22°C) the β_1-injected embryos displayed abnormal development as described above. To examine the toxicity and specificity of MOs themselves for target genes, we injected 4 base mispaired MO (β1-4 mis MO) or coinjected mRNA coding each subunit of soluble GC to embryos with MOs, resulting in no defect (data not shown).

DISCUSSION

In the present study, we obtained the clones of the cDNA fragments for *nNOS*, *OlGCS-α_2*, *cGK I*, and *cGK II*, all of which are NO/cGMP signaling pathway constituents, from medaka fish embryos, and then examined their temporal and spatial expression patterns. The deduced amino acid sequences of all of the clones were highly similar to those reported for the teleost, salmon and zebrafish corresponding, as well as to those reported for mammals (Fig. 2) (Nakane *et al*., 1993; Ogura *et al*., 1993; Holmqvist *et al*., 2000; Øyan *et al*., 2000). In a previous study, we isolated the full-length cDNAs for the medaka fish soluble GC α_1- and β_1- subunits (Mikami *et al*., 1998), and recently we obtained the full-length cDNA for the medaka fish soluble GC α_2-subunit (Yao, Y., Yamamoto, T., Suzuki, N., unpublished data). Therefore, we presume that the medaka fish NO/cGMP signaling pathway comprises the same components (NO synthase, soluble GCs, and cGMP-dependent protein kinases) found in mammals. In medaka fish, two genes, *OlGCS-β_1* and *nNOS*, both of which translation products are comprised in the NO/cGMP signaling pathway were expressed maternally, and the expression of *OlGCS-α_1* and *OlGCS-α_2*, both of which translation products are possible counterparts of OlGCS-β_1, was not detected until a later developmental stages (Fig. 3). Nevertheless, the b_1-MO injected embryos exhibited delay or inhibition of development in a dose-dependent manner (Fig. 6A-m, 6A-n). In this regard, it should be mentioned that an NOS inhibitor, N^G-nitro-L-arginine has been shown to inhibit the development in mammalian embryos (Gouge *et al*., 1998). Moreover, Chen *et al.* (2001) demonstrated that 8-Br-cGMP reversed the inhibitory effect of Nω-nitro-L-arginine methyl ester (L-NAME) and rescued the growth of the embryo, and a soluble GC inhibitor, 1H-[1, 2, 4] Oxadiazolo [4, 3-a] quinoxalin-1-one (ODQ), inhibited the development in a dose-dependent manner. These facts indicate that the NO/cGMP signaling pathway plays some important roles in early embryonic development of mammals. However, in our present study, no expression of *OlGCS-α_1* or *OlGCS-α_2* was detected in the early developmental stages of medaka fish. Therefore, we presume that there are unknown soluble GC activation systems involving NO without the alpha subunits.

Both the *OlGCS-α_1* and *OlGCS-β_1* transcripts were colocalized in the whole brain in the 7-day (stage 37) and 9-day hatched embryos (stage 39) (Fig. 4). This finding was coincident with our previous study, in which GFP fluorescence was detected in the brain when a *OlGCS-α_1* promoter-GFP fusion gene construct was injected into medaka fish 2-cell stage embryos (Mikami *et al*., 1999). The signals due to both transcripts were detected in the whole embryo in the early developmental stages, and then became gradually localized mainly in the brain as development continued. Harteneck *et al*. (1991) identified the soluble GC α_2-subunit mRNA in the human fetal brain. Recently, Gibb and Garthwaite (2001) demonstrated that the α_2 transcripts are widely distributed throughout the developing rat brain, and are abundant in the cerebellum and hippocampus. Similarly, in medaka fish the signals due to the *OlGCS-α_2* transcript were detected in the brain of the 4-day-old embryos, but they were dim in the early embryo as in the cases of the *OlGCS-α_1* and *OlGCS-β_1* transcripts (Fig. 4). In contrast, the signals due to *nNOS* and *cGK I* were restricted, suggesting that the transcripts of both genes function in limited sites.

Although, there have been many papers on the gene

expression patterns of the NO/cGMP signaling pathway components, most of them have focused on the expression in adult organs, and there have have been few reports, dealing with the embryonic expression of these genes. In the present study, we found that *nNOS* was expressed in the tail during the somitegenesis stage and then became expressed in the otic vesicles and brain ventricle (Fig. 5A). It has been reported that the activity of NOS was dependent on Ca^{2+}/Calmodulin (CaM), and that the localization of calcium pulse is dynamically changed throughout zebrafish embryonic development (Creton *et al*., 1998; Gilland *et al*., 1999). Our results demonstrated that the change of the expression pattern of *nNOS* in the medaka fish embryos was parallel to the calcium transitions. Calcium signaling throughout the segmentation period was also evedent in the tail bud, coincident with the *nNOS* expression pattern. Moreover, the α_2-MO injected embryos displayed the degenerated cells in the tail at stage 22 (Fig. 6B-j, arrow), suggesting that the NO/cGMP signaling pathway plays novel roles in the tail bud throughout the somitegenesis period. Our results that NOS was expressed in the otic vesicles after stage 22 (Fig. 5A) and that the otic vesicles were enlarged in the α_1-MO injected embryos (arrowheads in Fig. 6A-h and 6B-f) also suggest that the NO/cGMP signaling pathway involves in the formation of the otic vesicles.

It has been reported that iNOS plays a role in the immune system in mammals (Chartrain *et al*., 1994) and it has been proposed that PDE2 involves in thymocyte differentiation (Michie *et al*., 1996), probably via the following cascade: iNOS activates soluble GC, which then synthesizes cGMP, which in turn participates in the signal transduction through effector such as PDE2 and cGK I. In salmon, it is known that *iNOS* is expressed in the thymus (Øyan *et al*., 2000). In the present study, we were unable to obtain the cDNA fragment for either iNOS or eNOS, and thus did not determine their expression sites. However, our results demonstrated that the transcripts of *cGK I*, a downstream modulator, in the NO/cGMP signaling pathway, were detected in the thymus of medaka fish embryos (Fig. 5B), suggesting that the signal transduction similar in mammalian thymocyte differentiation and salmon thymus function in the medaka fish embryonic differentiation.

Using an immunohistochemical method, Zhan *et al*. (1999) demonstrated that *eNOS* and *cGK I* were expressed in rat lung and suggested the presence of an NO/cGMP signaling pathway in the respiratory ciliated epithelia of the rat lung. Our finding that *cGK I* was expressed at the medaka fish gill arch may indicate that the NO/cGMP signaling pathway plays an important role in the respiratory organ of medaka fish. Despite our many efforts, however, we were unable to detect another cGK isoform, *cGK II*, by *in situ* hybridization in any of the developmental stages of medaka fish embryos examined, suggesting that cGK II, unlike cGK I, does not play a role in developmental events.

In this study, we detected the expression of *nNOS* and *cGK I* in the spinal floor plate and DRG of 5-day-old embryos by section *in situ* hybridization (Fig. 5A-e, arrow; 5B-e, arrowhead). It has been reported that *nNOS* and *cGK I* were expressed in the small- and medium-diameter DRG neurons and spinal floor plate of mouse embryos (Bredt and Snyder, 1994; Qian *et al*., 1996) and both effectors have been shown to participate in neuronal differentiation (Peunova and Enikolopov, 1995) and axon outgrowth (Hess *et al*., 1993). In addition, the signals in the lateral spinal cord (Fig. 5A-e, arrowhead) may be reflected in the fact that nNOS was expressed in axonal projection to the dorsal spinal cord (Qian *et al*., 1996). It has been proposed that cGMP enhances the sonic hedgehog response in the spinal cord, while cAMP blocks the hedgehog pathway through cAMP-dependent protein kinase (cAK) (Jiang and Struhl, 1995; Robertson *et al*., 2001). Moreover, Scott and Jennes (1991) demonstrated that atrial natriuretic peptide (ANP) binds to the cells in the dorsal and ventral neural tube, suggesting that, in addition to the NO/cGMP signaling pathway, the NPs/cGMP signaling pathway also participates in the dorsal-ventral patterning in the neural tube, further indicating the complexity of the crosstalk among the various signaling pathways. Several papers have suggested that NO in the CNS may play roles in synaptogenesis, axon guidance, axon outgrowth and long-term potentiation (LTP) in the cerebellum (Izumi *et al*., 1992; Williams *et al*., 1994). In the present study, we demonstrated the malformation of notochord and somite border in the soluble GC knock-down embryos due to MO injection (arrows and arrowheads in Fig. 6B-e and 6B-h). We presume that these abnormalities of the CNS were caused by cell death and the malformation of synaptic connections owing to the block of the NO/cGMP signaling pathway in the CNS. However, Huang *et al*. (1993) reported that the phenotypes of *nNOS* knock-out mice were almost normal, and that the mice showed no histopathological abnormalities other than enlarged stomach; they suggested that this phenotypic normalcy was probably due to compensation by the other NOS isoforms. Judging from our results, on the other hand, the disruption of the soluble GC subunit gene in mammals seems to cause severe defects which may lead to difficulty in analyzing the events throughout the embryogenesis. This latest loss-of-function technology using medaka fish embryos makes it much easier to investigate the novel roles of the NO/cGMP signaling pathway in embryogenesis. Further studies will be needed to clarify the novel target molecules in this pathway.

ACKNOWLEDGEMENTS

The authors would like to thank Ms. H. Kuboshita for culturing of medaka fish and the staff members of the Center for the Advanced Sciences and Technology, Hokkaido University for the use of their laboratory facilities. This work was supported in part by a Grant-in-Aid for Scientific Research from the Ministry of Education, Science, Sports, and Culture of Japan (no. 11236202), the Japan Society for the Promotion of Science (no. 13010976) and National Project on Protein structural and Functional Analyses.

REFERENCES

Bredt DS,Snyder SH (1994) Transient nitric oxide synthase neurons in embryonic cerebral cortical plate, sensory glia, and olfactory epithelium. Neuron 13: 301–313

Butt E, Geiger J, Jarchau T, Lohmann SM, Walter U (1993) The cGMP-dependent protein kinase-gene, protein, and function. Neurochem Res 18: 27–42

Chartrain NA, Geller DA, Koty PP, Sitrin NF, Nussler AK, Hoffman EP, Billiar TR, Hutchinson NI, Mudgett JS (1994) Molecular cloning, structure, and chromosomal localization of the human inducible nitric oxide synthase gene. J Biol Chem 269: 6765–6772

Chen H-W, Jiang W-S, Tzeng C-R (2001) Nitric oxide as a regulator in preimplantation embryo development and apoptosis. Fertil Steril 75: 1163–1171

Creton R, Speksnijder JE, Jaffe LF (1998) Pattern of free calcium in zebrafish embryos. J Cell Sci 111: 1613–1622

Gibb BJ, Garthwaite J (2001) Subunits of the nitric oxide receptor, soluble guanylyl cyclase, expressed in rat brain. Eur J Neurosci 13: 539–544

Gilland E, Miller AL, Karplus E, Baker R, Webb AE (1999) Imaging of multicellular large-scale rhythmic calcium waves during zebrafish gastrulation. Proc Natl Acad Sci USA 96: 157–161

Gouge RC, Marshburn BE, Gohdon BE, Nunley W, Huet-Hudson YM (1998) Nitric oxide as a regulator of embryonic development. Biol Reprod 58: 875–879

Hall AV, Antoniou H, Wang Y, Cheung AH, Arbus AM, Olson SL, Lu WC, Kau CL, Marsden PA (1994) Structural organization of the human neuronal nitric oxide synthase (NOS1). J Biol Chem 269: 33082–33090

Harteneck C, Wedel B, Koesling D, Malkewitz J, Böhme E, Schultz G (1991) Molecular cloning and expression of a new alpha-subunit of soluble guanylyl cyclase. Interchangeability of the alpha-subunits of the enzyme. FEBS Lett 292: 217–222

Hess DT, Patterson SI, Smith DS, Skene JH (1993) Neuronal growth cone collapse and inhibition of protein fatty acylation by nitric oxide. Nature 366: 562–565

Holmqvist B, Ellingsen B, Alm P, Forsell J, Oyan A-M, Goksoyr A, Fjose A, Seo H-C (2000) Identification and distribution of nitric oxide synthase in the brain of adult zebrafish. Neurosci Lett 292: 119–122

Huang PL, Dawson TM, Bredt DS, Snyder SH, Fishman MC (1993) Targeted disruption of the neuronal nitric oxide synthase gene. Cell 75: 1273–1286

Huang PL, Huang Z, Mashimo H, Bloch KD, Moskowitz MA, Bevan JA, Fishman MC (1995) Hypertension in mice lacking the gene for endothelial nitric oxide synthase. Nature 377: 239–242

Iwamatsu T (1994) Stages of normal development in the medaka *Oryzias latipes*. Zool Sci 11: 825–839

Izumi Y, Clifford DB, Zorumski CF (1992) Inhibition of long-term potentiation by NMDA-mediated nitric oxide release. Science 257: 1273–1276

Jiang J, Struhl G (1995) Protein kinase A and hedgehog signaling in *Drosophila* limb development. Cell 80: 563–572

Koesling D, Herz A, Gausepohl H, Niroomand F, Hinsch K-D, Mulsh A, Böhme E, Schultz G, Frank R (1988) The primary structure of the 70 kDa subunit of bovine soluble guanylate cyclase. FEBS Lett 239: 29–34

Koesling D, Harteneck C, Humbert P, Bosserhoff A, Frank R, Schultz G, Böhme E (1990) The primary structure of the larger subunit of soluble guanylyl cyclase from bovine lung. Homology between the two subunits of the enzyme. FEBS Lett 266: 128–132

Kusakabe T, Suzuki N (2000) The guanylyl cyclase family in medaka fish *Oryzias latipes*. Zool Sci 17: 131–140

Lee TC, Zhao YD, Courtman DW, Steward DJ (2000) Abnormal aortic valve development in mice lacking endothelial nitric oxide synthase. Circulation 101: 2345–2348

Lucas KA, Pitari GM, Kazerounian S, Ruiz-Stewart I, Park J, Schulz S, Chepenik KP, Waldman SA (2000) Guanylyl cyclases and signaling by cyclic GMP. Pharmacol Rev 52: 375–414

MacMicking JD, Nathan C, Hom G, Chartrain N, Fletcher DS, Trumbauer M, Stevans K, Xie Q-W, Sokol K, Hutchinson N, Chen H, Mudgett JS (1995) Altered responses to bacterial infection and endotoxic shock in mice lacking inducible nitric oxide synthase. Cell 81: 641–650

Markert T, Vaandrager AB, Gambaryan S, Pohler D, Hausler C, Walter U, De Jonge HR, Jarchau T, Lofmann SM (1995) Endogenous expression of type II cGMP-dependent protein kinase mRNA and protein in rat intestine. Implications for cystic fibrosis transmembrane conductance regulator. J Clin Invest 96: 822–830

Marsden PA, Heng HHQ, Scherer S, Stewart RJ, Hall AV, Shi XM, Tsui LC, Schappert KT (1993) Structure and chromosomal localization of the human constitutive endothelial nitric oxide synthase gene. J Biol Chem 268: 17478–17488

Michie AM, Lobban M, Muller T, Harnett MM, Houslay MD (1996) Rapid regulation of PDE-2 and PDE-4 cyclic AMP phosphodiesterase activity following ligation of the T cell antigen receptor on thymocites: analysis using the selective inhibitors erythro-9-(2-hydroxy-3-nonyl)-adenine (EHNA) and rolipram. Cell Signal 8: 97–110

Mikami T, Kusakabe T, Suzuki N (1998) Molecular cloning of cDNAs and expression of mRNAs encoding alpha and beta subunits of soluble guanylyl cyclase from medaka fish *Oryzias latipes*. Eur J Biochem 253: 42–48

Mikami T, Kusakabe T, Suzuki N (1999) Tandem organization of medaka fish soluble guanylyl cyclase α_1 and β_1 subunit genes. Implications for coordinated transcription of two subunit genes. J Biol Chem 274: 18567–18573

Nakane M, Schmidt HHHW, Pollock JS, Förstermann U, Murad F (1993) Cloned human brain nitric oxide synthase is highly expressed in skeletal muscle. FEBS Lett 316: 175–180

Nasevicius A, Ekker SC (2000) Effective target gene 'Knockdown' in zebrafish. Nat Genet 26: 216–220

Ogura T, Yokoyama T, Fujisawa H, Kurashima Y, Esumi H (1993) Structure diversity of neuronal nitric oxide synthase mRNA in the nervous system. Biochem Biophys Res Commun 193: 1014–1022

Øyan A-M, Nilsen F, Goksoyr A, Holmqvist B (2000) Partial cloning of constitutive and inducible nitric oxide synthases and detailed neuronal expression of NOS mRNA in the cerebellum and optic tectum of adult Atlantic salmon (*Salmo salar*). Mol Brain Res 78: 38–49

Peunova N, Enikolopov G (1995) Nitric oxide triggers a switch to growth arrest during differentiation of neuronal cells. Nature 375: 68–73

Pfeifer A, Aszódi A, Seidler U, Ruth P, Hofmann F, Fässler R (1996) Intestinal secretory defects and dwarfism in mice lacking cGMP-dependent protein kinase II. Science 274: 2082–2086

Pfeifer A, Klatt P, Massberg S, Ny L, Sausbier M, Hirneiβ C, Wang G-X, Korth M, Aszódi A, Andersson K-E, Krombach F, Mayerhofer A, Ruth P, Fässler R, Hofmann F (1998) Defective smooth muscle regulation in cGMP kinase I-deficient mice. EMBO J 17: 3045–3051

Qian Y, Chao DS, Santillano DR, Cornwell TL, Nairn AC, Greengard P, Lincoln TM, Bredt DS. (1996) cGMP-dependent protein kinase in dorsal root ganglion: relationship with nitric oxide synthase and nociceptive neurons. J Neurosci 16: 3130–3138

Robertson CP, Gibbs SM, Roelink H (2001) cGMP enhances the sonic hedgehog response in neural plate cells. Dev Biol 238: 157–167

Russwurm M, Behrends S, Harteneck C, Koesling D (1998) Functional properties of a naturally occurring isoform of soluble guanylyl cyclase. Biochem J 335: 125–130

Sanger F, Nicklen S, Coulson AR (1977) DNA sequencing with chain-terminating inhibitors. Proc Natl Acad Sci USA 74: 5463–5467

Schmidt HHHW, Walter U (1994) NO at work. Cell 78: 919–925

Scott JN, Jennes L (1991) Localization of ^{125}I-atrial natriuretic peptide (ANP) in the rat fetus. Anat Embryol 183: 245–249

Wei X-Q, Charles IG, Smith A, Ure J, Huang F-P, Xu D, Muller W, Moncada S, Liew FY (1995) Altered immune responses in mice lacking inducible nitric oxide synthase. Nature 375: 408–411

Wernet W, Flockerzi V, Hofmann F (1989) The cDNA of the two isoforms of bovine cGMP-dependent protein kinase. FEBS Lett 251: 191–196

Williams CV, Nordquist D, McLoon SC (1994) Correlation of nitric oxide synthase expression with changing patterns of axonal projections in the developing visual system. J Neurosci 14: 1746–1755

Yamagami S, Suzuki K, Suzuki N (2001) Expression and exon/intron organization of two medaka fish homologs of the mammalian guanylyl cyclase A. J Biochem 130: 39–50

Yamamoto T, Suzuki N (2002) Promoter activity of the 5'-flanking region of medaka fish soluble guanylyl cyclase α_1 and β_1 subunit gene. Biochem J 361: 337–345

Yuen PST, Potter LR, Garbers DL (1990) A new form of guanylyl cyclase is preferentially expressed in rat kidney. Biochemistry 29: 10872–10878

Zhan X, Li D, Johns RA (1999) Immunohistochemical evidence for the NO cGMP signaling pathway in respiratory ciliated epithelia of rat. J Histochem Cytochem 47: 1369–1374

(Received November 9, 2002 / Accepted November 30, 2002)